# Application of Model-based Design Approach on Dynamic Tensile Testing of Carbon/Epoxy Composites at Intermediate Strain Rates

## Sanghyun Yoo[1,2*], Euiyoul Kim[3], Nathalie Toso[1], Heinz Voggenreiter[1]

[1]Institute of Structures and Design, German Aerospace Center,
Pfaffenwaldring 38-40, 70569 Stuttgart, Germany
[2]Innovation Center for Small Aircraft Technologies, German Aerospace Center,
Campus-Boulevard 79, 52074 Aachen, Germany
[3]Faculty of Civil and Environmental Engineering, University of Stuttgart,
Pfaffenwaldring 7, 70569 Stuttgart, Germany
* Sanghyun.Yoo@dlr.de

**Keywords:** Strain rate effects; Model-based Design (MBD); Parameter identification;

**Summary:** *The reliable strain rate-dependent material properties at intermediate strain rate levels (1-200 s^-1) are crucial for an accurate crashworthy design of fibre-reinforced polymer (FRP) composite structures. However, the presence of unacceptable oscillations in measured force signals hinders the precise identification of the dynamic mechanical response of materials. The current work reports the results of gained in an initial study using a novel numerical model developed through a Model-based Design (MBD) approach. A multi-degree-of-freedom (MDOF) mass-spring-damper model is employed to investigate the dynamic characteristics of a whole experimental test setup to gain insights into the dynamic interaction between the test machine and the test specimen. The developed model was calibrated by the results from dynamic tension testing of Aluminium Alloy 2024-T3. Then, the model parameters were optimised using a genetic algorithm (GA). Subsequently, the adaptability of the developed model to carbon/epoxy composites, IM7/8552, was examined. The proposed model is promising to identify the influence of the test setup on the measurements and effectively distinguish excessive oscillations caused by its inertial effect at intermediate strain rate levels. The model will offer a robust solution to identify oscillations and, therefore, expand the testing capabilities to a broader range of strain rates.*

## 1 INTRODUCTION

In dynamic tensile testing, an impulse-like loading is applied to the test specimen through a slack adapter, resulting in high amplitude stress waves and excitation of the test system at its natural frequency. Consequently, measured force signals are superimposed with high amplitude oscillations, known as system ringing [1-4]. The magnitude of the generated oscillations is strongly affected by the vibrational behaviours of the experimental test setup and the dynamic responses of the test machine [2, 3]. Therefore, capturing the dynamic characteristics of an experimental setup is crucial in dynamic testing at intermediate strain rates to reduce the system ringing and, thus, to ensure accurate and reliable test results.

Several improvements to handle the system ringing have been implemented to the test fixture [5-7] or the test specimen [8-11], as well as the application of signal processing techniques [12-16]. Furthermore, a mass-spring-damper model has been utilised to approximate the experimental setup and evaluate the test system's natural frequency, which is

crucial in controlling system ringing [2, 7, 16].

The main objective of this study is to capture the dynamic characteristics of an entire experimental setup using a multi-degree-of-freedom (MDOF) mass-spring-damper model so that the mechanical material behaviours of the test specimen can be reliably "cleaned" from the experimental setup's influences and the system ringing. To that aim, a physics-based analysis described in Fig. 1 is developed to accurately measure the force applied to the specimen during the test and therefore reliably extract the material properties in the short-time dynamic regime.
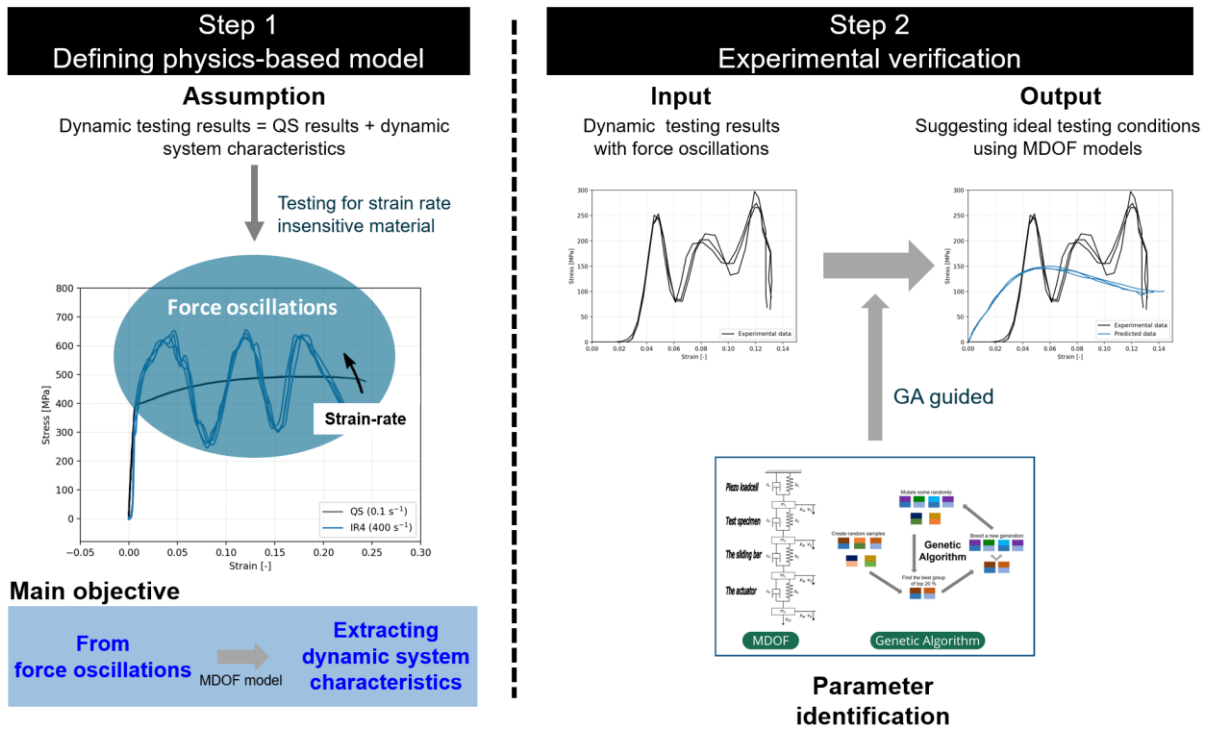


Figure 1: A physics-based analysis strategy for identifying/extracting system ringing in dynamic tension testing using the MDOF model and a genetic algorithm.

## 2 MATERIALS AND EXPERIMENTAL METHODS

### 2.1 Materials

Flat sheets of Aluminium-Alloy 2024-T3 (later denoted as AA) were cut into given geometries with a water-jet cutter along the rolling direction. The dog-bone specimens suggested by Lefford N. et al. [17] with a gauge length of 10 mm were used. Dynamic testing system's responses could be extracted by a basic assumption that Aluminium Alloy 2024-T3 is a strain rate insensitive material at intermediate strain rates [18] so that the observed high amplitude oscillations caused by the test machine and fixture could be quantitatively evaluated from quasi-static test results. Further validation of the method was performed by using in-plane shear results of carbon/epoxy composites, IM7/8552 (later denoted as CC) at intermediate strain rates, which were obtained from the literature [19].

## 2.2 Experimental Methods

### 2.2.1 Dynamic testing using a high-speed servo-hydraulic machine

Dynamic tensile tests were carried out at strain rates from 0.1 to 200 s$^{-1}$, and namely at nominal strain rates of 0.1, 10, 100, and 200 s$^{-1}$. The high-speed servo-hydraulic testing machine, an Instron® VHS 100/20, was used with a piezo-electric load cell with a capacity of ± 120 kN (Kistler-9317B from Kistler Instrumente GmbH, Germany). The force signals were amplified with a Kistler type 5011B charge amplifier.

Digital Image Correlation (DIC) was used in combination with a high-speed camera (FASTCAM SA-Z from Photron®, Japan) to obtain the strain fields and strain rates with a spatial resolution of about 50 µm/pixel. Random black-on-white speckle patterns were applied using an airbrush onto the specimen surfaces, and the average speckle size was about 40 µm. High speed images were synchronised with the force signal obtained with a National Instrument Data Acquisition system, NI-DAQ (USB-6251 BNC from National Instruments™, USA). Images were post-processed with the GOM® Correlate software. The DIC strain field was used to identify the necking and fracture location within the gauge section. Then, strain and strain rate were extracted from the virtual extensometer with 6 mm gauge length, which located close to the fracture surface to cover the necking area.

### 2.2.2 Experimental modal analysis (EMA)

The EMA test was conducted with two ICP® accelerometers (352A71 from PCB Piezotronics, Inc.) that had a sensitivity of 1.02 mV/g. The excitation impulses were provided by an ICP® impact hammer (Model 086C01 from PCB Piezotronics, Inc). The hammer had a sensitivity of 11.2 mV/N and was equipped with a hard metal tip. The data acquisition system was a multi-channel VibPilot from M+P international with a sampling rate of 100 kHz. An average of 3 impact tests was used. The impact location was selected at the bottom of the loadcell, and it was impacted in the vertical direction to represent the axial loading direction.

## 3  MODEL BASED NUMERICAL MODEL

### 3.1 Description of the numerical model

A 4-DOF model is implemented to provide a more detailed representation of the short-time transient behaviours of an entire test system, including a high-speed testing machine, a slack adapter, a piezo-electric loadcell and a test specimen. The MDOF model allows for interpreting vibrational responses in the test specimens by considering a dynamic interaction with the test setup. In addition, the use of this model enables the estimations of the individual dynamic responses of the test machine, fixture and specimen.

Fig. 2 describes a parameter identification strategy for the 4-DOF model. The input parameters are calibrated for optimal performance using quasi-static test results. A schematic of the MDOF model constructed with multiple masses, springs, and dampers for the dynamic testing system is shown in Fig. 2 (c). Table 1 summarises detailed information on the dynamic test system, which consists of 4 representative components with an initial estimation of lumped masses and spring constants.
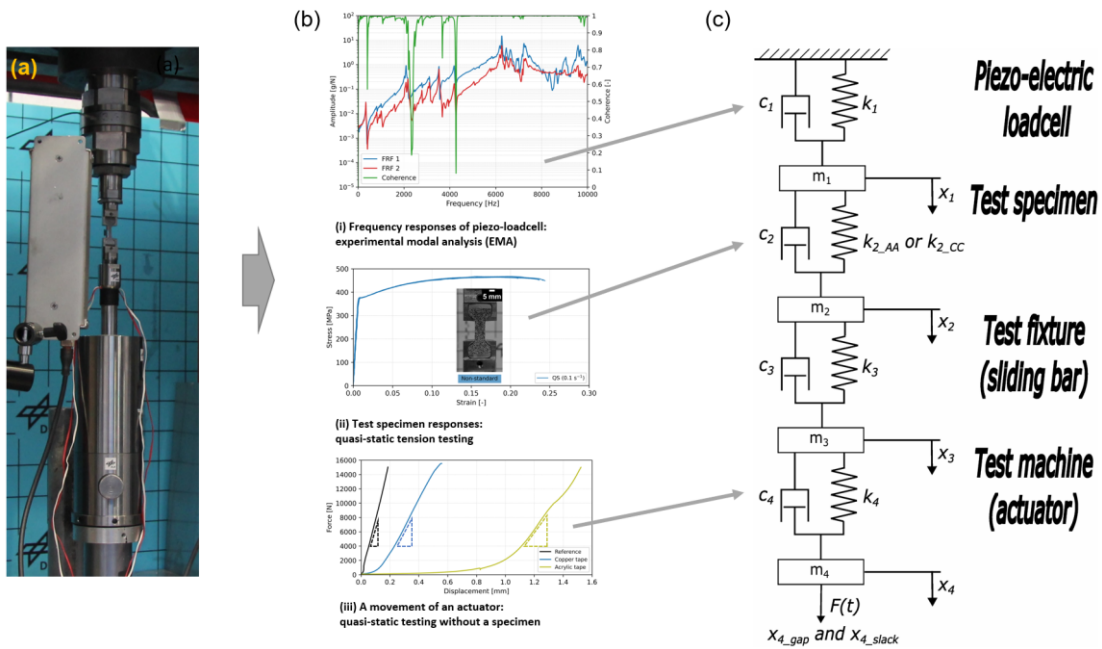
Figure 2: (a) Experimental test setup with a slack adapter, (b) Diagram for initial input parameters; (b-i) experimental modal analysis by impact hammer for piezo-electric loadcell, (b-ii) quasi-static data of Aluminium alloy 2024- T3, (b-iii) influence of damping materials on load introduction at the quasi-static condition without the specimen, (c) Dynamic responses of the 4-DOF mass-spring-damper model.

Table 1: Detailed information of the dynamic testing system and its initial estimation of lumped masses and spring constant.

| # | Represented components | Actual components | Mass, $m$ [kg] | Spring constant, $k$ [N/m]* |
|---|---|---|---|---|
| 1 | Piezo-electric loadcell | Loadcell**, adapter, and upper grip | 7.9 | $8.4 \times 10^9$ |
| 2 | Test specimen | Specimen, and lower grip | 0.14 | $4.4 \times 10^8$ |
| 3 | Test fixture (sliding bar) | Sliding bar and cone | 0.48 | $6.47 \times 10^9$ |
| 4 | Test machine (actuator) | Damping, sleeve, base, and piston | 37.4 | $8.55 \times 10^8$ |

* spring constant is estimated with an equation $k = EA/L$.

** values are obtained from the manufacturer.

In the model, the movement of the actuator is defined based on an exponential curve fitting with two hyperparameters ($x_{4\_gap}$ and $x_{4\_slack}$) followed by a linear behaviour (Fig. 2 (b-iii)). The model assumes that the propagation of stress waves in the test setup can be treated as one-dimensional while neglecting lateral inertia and time-invariant problems. Analytical solutions of this model are calculated by solving ordinary differential equations (ODEs) shown in equations 1 to 4. Those ODEs are numerically solved using the 'odeint' function from the SciPy library (version 1.9.3). The final solutions are then compared and validated to experimental test results obtained from a wide range of strain rates and damping conditions. ODEs describing the test system are:

$$m_1\ddot{y}_1 = -c_1\dot{y}_1 - k_1 y_1 - k_2(y_1 - y_2) \tag{1}$$

$$m_2\ddot{y}_2 = -k_2(y_2 - y_1) - c_3(\dot{y}_2 - \dot{y}_3) - k_3(y_2 - y_3) \tag{2}$$

$$m_3\ddot{y}_3 = -c_3(\dot{y}_3 - \dot{y}_2) - k_3(x_3 - x_2) - c_4(\dot{y}_3 - \dot{y}_4) - k_4(x_3 - x_4) \tag{3}$$

$$m_4\ddot{y}_4 = -c_4(\dot{y}_4 - \dot{y}_3) - k_4(x_4 - x_3) + F_{(t)} \tag{4}$$

where $m_{i-th}$ = mass, $c_{i-th}$ = damping, $k_{i-th}$ = stiffness constant, and $F_{(t)}$ = hydraulic force shown in Fig. 2(b-iii).

## 3.2 Numerical curve fitting of the test specimen

A curve fitting is performed to parameterise the material behaviour curve of the test specimen and to identify the input model parameter, $k_2$. To that aim, the quasi-static test results are used to define the characteristics of the test specimen without implementing complex constitutive models. The determination of the elastic-viscoplastic behaviour of metallic materials undergoing dynamic tension requires converting the engineering force–displacement data into true curves. The elastic-viscoplastic behaviour is divided into two zones, for each of which the fitted parameters are determined. While the elastic response is defined with a linear function, the viscoplastic response is expressed with a 3rd order polynomial function (Fig. 3(a)) [20]. The extracted parameters of the linear and polynomial functions are then used for the MDOF model in order to fit the quasi-static material curve of the material mode. The aforementioned approach including the combination of linear and nonlinear relationships is used again to represent the quasi-static response of the carbon-epoxy composite specimen (Fig. 3(b)). The only difference is the viscous response, which is expressed with a 5th order polynomial function. Both $R^2$ values from curve fitting are found to be 0.999, indicating an excellent fit between the fitting curve and the experimental data.
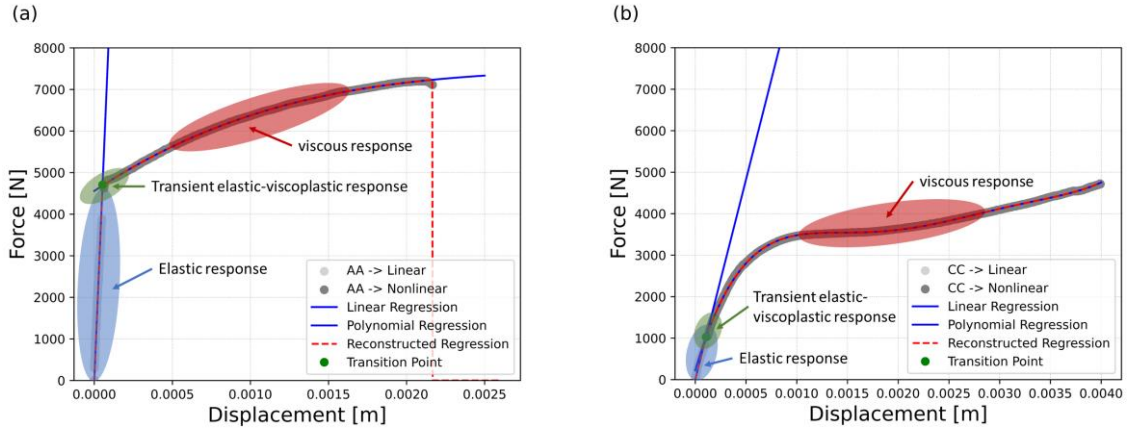


Figure 3: Numerical curve fitting from quasi-static test results of (a) Aluminium Alloy 2024-T3 (AA) and (b) carbon-epoxy composites (CC).

## 3.3 Calibration of the piezo-electric loadcell

The calibration of a piezo-electric load cell involves evaluating its natural frequency to understand its dynamic behaviours accurately. The natural frequency of the test system can be determined from dynamic testing of a brittle material, as described in [2]. The dynamic tension testing of a brittle material was performed (Fig. 4(a)), and the force-time data after fracture was converted to a power spectral density (PSD) using the fast Fourier transform (FFT) method.

Analysis of the PSD data (Fig. 4(b)) reveals a dominant natural frequency of approximately 5200 Hz. Furthermore, the amplitude of oscillations in the force signals is primarily influenced by the structure of the upper part of the test machine, including the piezo-electric loadcell, the upper grips and the crosshead. This observation aligns with findings reported in the literature [21]. To further investigate the dynamic response of the upper part of the test machine, the EMA was conducted. The EMA results (Fig. 2(b-i)) demonstrate good agreement with the natural frequency determined from the PSD data.

To estimate the dynamic behaviour of piezo-electric loadcell, a SDOF (single-degree-of-freedom) model with mass ($m_1$), damper ($c_1$), and spring constants ($k_1$) is utilized. The governing ODE is formulated and then solving it numerically using an ODE solver to accurately capture the dynamics of the test system. In the calibration process, the damping coefficient ($c_1$) in the SDOF model is adjusted to match the damped dynamic responses obtained from the PSD data, while $m_1$ and $k_1$ are kept fixed. Hence, the calibration of the loadcell is performed by considering the natural frequency and dynamic characteristics of the test system.
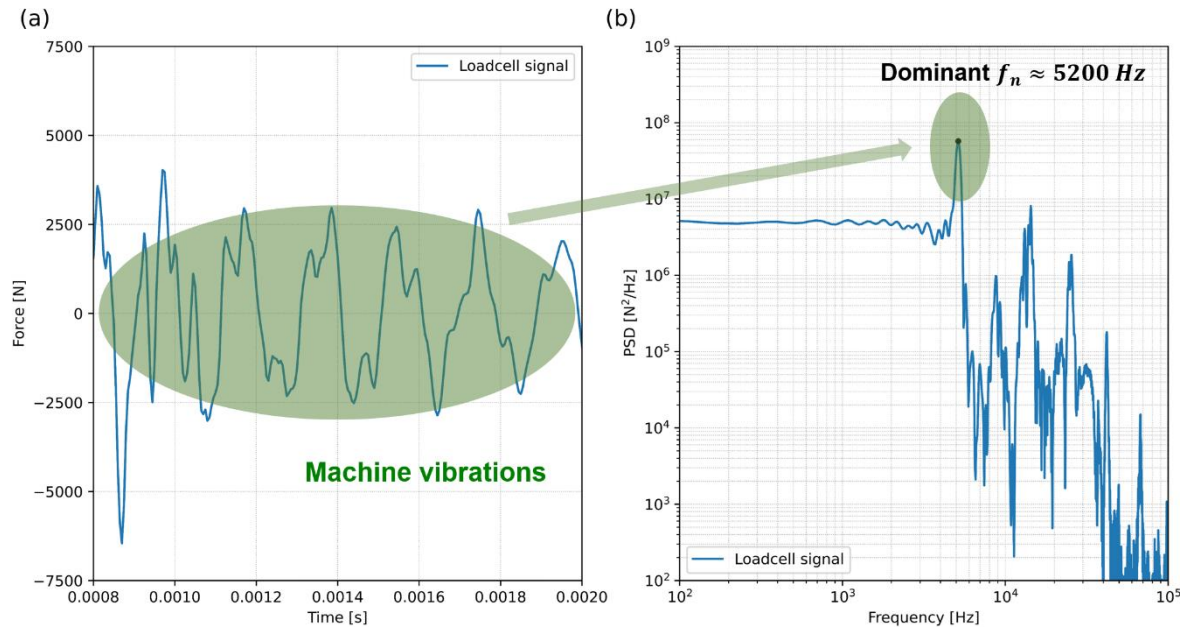


Figure 4: Calibration of the piezo-electric loadcell: (a) Dynamic force-time data after a brittle material is fractured, and (b) the dominant natural frequency ($f_n$), determined from power spectral density.

## 4 DYNAMIC TEST SYSTEM MODEL VALIDATION

### 4.1 Parameter identification for the MDOF model

The genetic algorithm (GA) is a bio-inspired stochastic search algorithm motivated by the process of natural selection and genetics [22, 23]. Its key idea is to simulate the process of natural selection by creating a population of candidate solutions, evaluating their fitness, and breeding them to generate new generations of solutions that have a higher probability of achieving the desired outcome. In this study, the GA for data-driven optimisation is implemented to find an optimal set of model parameters that best fit experimental data and initial reference parameters. Firstly, the GA approach involves the generation of an initial population of potential solutions (i.e., a set of model parameters). Secondly, the fitness of each

population is evaluated by comparing the model output with the experimental data. Thirdly, $R^2$ is calculated to measure the proportion of the variance in the experimental data. Finally, a loss function based on the $1-R^2$ value is used to assess the convergence of the model by comparing the predicted model against experimental force-displacement data. By minimising the $1-R^2$ value, the ODE solver can be fine-tuned to achieve a better fit between predicted values and the experimental data. Defined input parameters from the GA optimisation process are given in Table 2.

Table 2. Defined input parameters of the MDOF model for using the GA (quasi-static condition without damping condition).

| Represented components | | Calibrated input parameter* |
| --- | --- | --- |
| Piezo-electric loadcell (section 3.3) | $k_1$ | 8.40E+09 |
| | $C_1$ | 5.51E+05 (before fracture) 9.22E+03 (after fracture) |
| Test specimen (section 3.2) | $k_{2\_AA}$ | Linear: 8.63E+07 Nonlinear $= A \cdot x^3 + B \cdot x^2 + C \cdot x + D$ A = 1.36E+11 B = -9.26E+08 C = 1.97E+06 D = 4.56E+03 |
| | $k_{2\_CC}$ | Linear = 9.05E+06 Nonlinear $= A \cdot x^5 + B \cdot x^4 + C \cdot x^3 + D \cdot x^2 + E \cdot x + F$ A = 6.32E+16 B = -7.83E+14 C = 3.69E+12 D = -8.08E+09 E = 8.17E+06 F = 2.40E+02 |
| | $C_2$ | 0 |
| Test fixture (section 3.1) | $k_3$ | 4.40E+08 |
| | $C_3$ | 0 |
| Test machine (section 3.1) | $k_4$ | Linear = 1.19E+08 Nonlinear $= A \cdot e^{B \cdot x} + C$ A = 4.43E+03 B = 4.87E+05 C = 1.94E+07 |
| | $C_4$ | 1.57E+04 |
| | $x_{4\_gap}$ | 1.87E-05 |
| | $x_{4\_slack}$ | 1.76E-06 |

* Unit: Spring constant, $k$ is in N/m and damping constant, $c$ is in N/(m/s). Also, $x_{4\_gap}$ and $x_{4\_slack}$ are in m.

7

## 4.2 Experimental validation

Fig. 5 compares the experimental and numerical results of the AA material without damping material obtained in the quasi-static regime and at the strain rate of 200 s⁻¹. It is clearly observed that both numerical results of AA show a good agreement with the experimental result. This indicates that the dynamic characteristics of the testing system are well described using the identified model parameters obtained with the GA. Furthermore, a similar agreement can be found for the results from CC in the quasi-static test conditions (Fig. 6(a)) when the same parameters are used.

On the other hand, identified parameters cannot predict the experimental result of the CC material at the strain rate of 200 s⁻¹ (Fig. 6(b)). This result reveals that the dynamic responses of fibre-reinforced plastic (FRP) composites differ from that of metallic material with increasing strain rates. It is assumed that the discrepancy is caused by the fact that the $k_{2\_CC}$ is not included with strain rate dependency. As an additional result, Fig. 6(b) shows that the use of damping material in the slack adapter enables mitigating the high amplitude oscillations. The comparison of the developed predicting model and the experimental data indicates that further investigations will have to be carried out to improve the overall optimisation procedure of the test specimen modelling as well as to integrate the effect of damping materials.
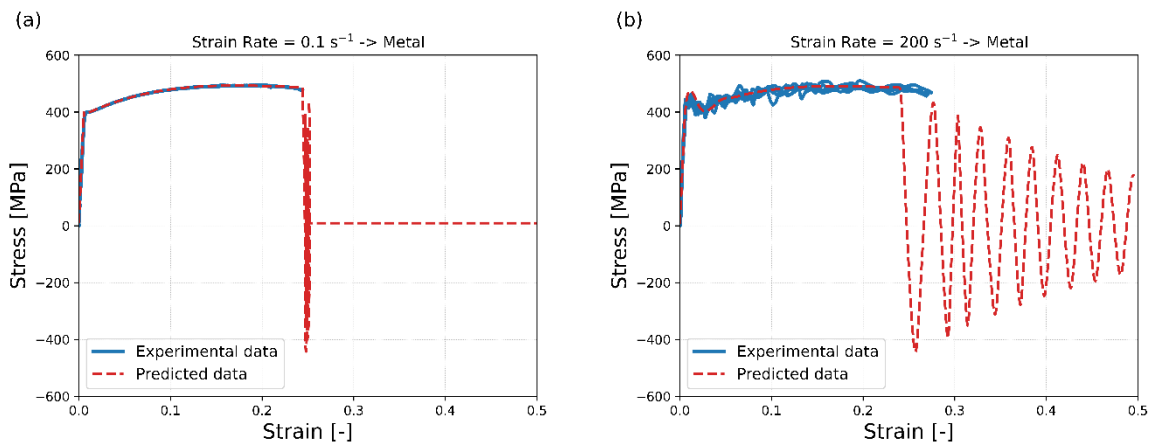


Figure 5: Experimental and numerical results of Aluminium Alloy 2024-T3 without damping: (a) at quasi-static condition, and (b) at strain rate of 200 s⁻¹.
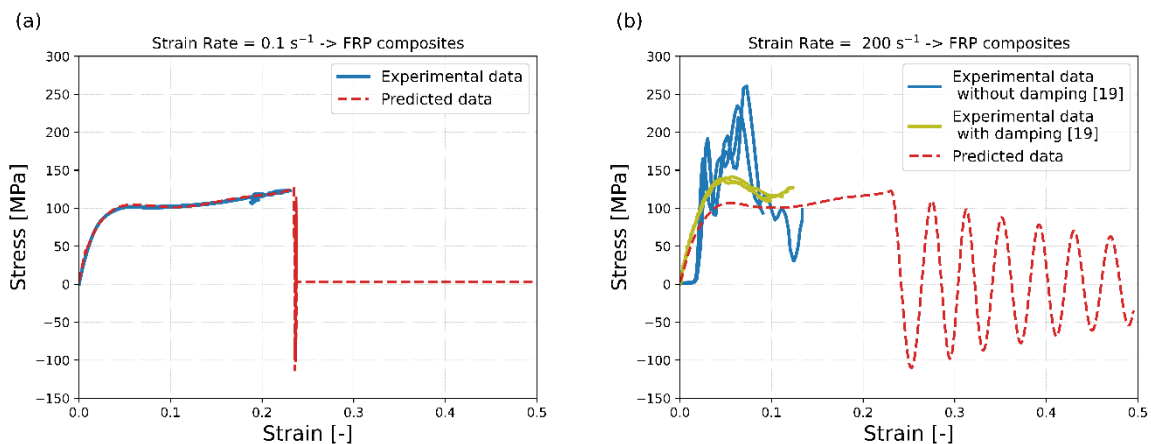


Figure 6: Experimental and numerical results of carbon/epoxy composites, IM7/8552: (a) at quasi-static condition without damping, and (b) at strain rate of 200 s⁻¹.

8

## 5 CONCLUSIONS

This study proposes the implementation of the 4-DOF model to analyse the dynamic performance of an entire experimental setup including the high-speed test machine, the slack adapter, the piezo-electric loadcell and the test specimen. The developed model is calibrated with the dynamic tension results of AA tested at various strain rates up to 200 s$^{-1}$. Also, it is possible to identify the optimal parameters to describe the dynamic test system behaviour by adjusting parameters using the GA. Using the MDOF model to understand the system ringing observed in the force measurement during the dynamic tension testing has proven to be a valuable approach.

However, further research is necessary to deeply investigate the limitations of the current methods and to develop more comprehensive models that account for the complexities of the dynamic material behaviours of FRP composites. To achieve this, machine learning algorithms like physics-informed neural networks (PINNs) will be implemented to improve the optimisation procedure. In the end, the main objective of those investigations is to improve the testing and postprocessing method to obtain reliable and reproducible dynamic test results with various materials at a broader range of strain rates.

## REFERENCES

[1] T. Bhujangrao, C. Froustey, E. Iriondo, F. Veiga, P. Darnis, F.G. Mata, Review of Intermediate Strain Rate Testing Devices, Metals 10(7) (2020) 894.
[2] X. Xiao, Dynamic tensile testing of plastic materials, Polymer Testing 27(2) (2008) 164-178.
[3] P. Larour, J. Noack, W. Bleck, Vibration Behaviour of Servohydraulic Dynamic Tensile Testing Machines, Materials Testing 51(4) (2009) 184-198.
[4] B.L. Boyce, M.F. Dilmore, The dynamic tensile behavior of tough, ultrahigh-strength steels at strain-rates from 0.0002s−1 to 200s−1, International Journal of Impact Engineering 36(2) (2009) 263-271.
[5] H. Huh, J.H. Lim, S.H. Park, High speed tensile test of steel sheets for the stress-strain curve at the intermediate strain rate, International Journal of Automotive Technology 10(2) (2009) 195-204.
[6] R. Othman, G. Gary, Testing Aluminum Alloy from Quasi-static to Dynamic Strain-rates with a Modified Split Hopkinson Bar Method, Experimental Mechanics 47(2) (2007) 295-299.
[7] Y. Xia, J. Zhu, K. Wang, Q. Zhou, Design and verification of a strain gauge based load sensor for medium-speed dynamic tests with a hydraulic test machine, International Journal of Impact Engineering 88 (2016) 139-152.
[8] J. Li, X. Fang, Stress Wave Analysis and Optical Force Measurement of Servo-Hydraulic Machine for High Strain Rate Testing, Experimental Mechanics 54(8) (2014) 1497-1501.
[9] A. Rusinek, R. Cheriguene, A. Bäumer, P. Larour, Dynamic behaviour of high-strength sheet steel in dynamic tension: Experimental and numerical analyses, The Journal of Strain Analysis for Engineering Design 43(1) (2008) 37-53.
[10] P. Wood, K.C., C. Schley, A., M. Williams, R. Beaumont, A. Rusinek, U. Mayer, A. Pearce, A method to calibrate a specimen with strain gauges to measure force over the full-force range in high rate testing, DYMAT - International Conference on the Mechanical and Physical Behaviour of Materials under Dynamic Loading 1 (2009) 265-273.
[11] X. Yang, L.G. Hector, J. Wang, A Combined Theoretical/Experimental Approach for

Reducing Ringing Artifacts in Low Dynamic Testing with Servo-hydraulic Load Frames, Experimental Mechanics 54(5) (2014) 775-789.

[12] X. Fang, A one-dimensional stress wave model for analytical design and optimization of oscillation-free force measurement in high-speed tensile test specimens, International Journal of Impact Engineering 149 (2021) 103770.

[13] C. Teena Mouni, P. Fayaz Khan, C. Ravishankar, S.A. Krishnan, S.K. Albert, Addressing the load-ringing phenomena observed at intermediate strain rates to obtain true material response using ensemble empirical mode decomposition, Materials Letters 325 (2022) 132778.

[14] P. Ying, W. Chen, Y. Ge, Q. Zhou, Y. Xia, Loading measurement for intermediate strain rate material test based on dynamic oscillation, International Journal of Impact Engineering 173 (2023) 104436.

[15] D. Zhu, B. Mobasher, S.D. Rajan, P. Peralta, Characterization of Dynamic Tensile Testing Using Aluminum Alloy 6061-T6 at Intermediate Strain Rates, Journal of Engineering Mechanics 137(10) (2011) 669-679.

[16] J. Klein, C. Hopmann, On the Origin and Handling of the Force Oscillation Phenomenon in Tensile Impact Testing of Polymer Materials, Experimental Mechanics 56(5) (2016) 749-758.

[17] N. Ledford, H. Paul, G. Ganzenmüller, M. May, M. Höfemann, M. Otto, N. Petrinic, Investigations on specimen design and mounting for Split Hopkinson Tension Bar (SHTB) experiments, EPJ Web of Conferences 94 (2015) 01049.

[18] J.D. Seidt, A. Gilat, Plastic deformation of 2024-T351 aluminum plate over a wide range of loading conditions, International Journal of Solids and Structures 50(10) (2013) 1781-1790.

[19] S. Yoo, D. Dalli, G. Catalanotti, N. Toso, F. Kessel, H. Voggenreiter, Dynamic intralaminar fracture toughness characterisation of unidirectional carbon fibre-reinforced polymer composites using a high-speed servo-hydraulic test set-up, Composite Structures 295 (2022) 115838.

[20] ISO 26203-2, Metallic materials — Tensile testing at high strain rates, Part 2: Servo-hydraulic and other test systems, International Organization for Standardization (ISO), 2011.

[21] D. Zhu, S.D. Rajan, B. Mobasher, A. Peled, M. Mignolet, Modal Analysis of a Servo-Hydraulic High Speed Machine and its Application to Dynamic Tensile Testing at an Intermediate Strain Rate, Experimental Mechanics 51(8) (2011) 1347-1363.

[22] B.M. Chaparro, S. Thuillier, L.F. Menezes, P.Y. Manach, J.V. Fernandes, Material parameters identification: Gradient-based, genetic and hybrid optimization algorithms, Computational Materials Science 44(2) (2008) 339-346.

[23] E. Kim, S. Hwang, S. Lee, Image-based approach to optimize the tyre pitch sequence for a reduction in the air-pumping noise based on a genetic algorithm, Proceedings of the Institution of Mechanical Engineers, Part D: Journal of Automobile Engineering 226(9) (2012) 1171-1184.